Finding the midline shift on CT and morph it back with a personal computer

Chun-Chih Liao

Department of Neurosurgery, Taipei Hospital, Department of Health
Graduate Institute of Medical Informatics, Taipei Medical University

Abstract

OBJECTIVE: Tracing the shifted midline on a slice of brain CT, 'pulling' it back into a straight line, and generating 'in-between' images with a personal computer.

METHODS: The upper and lower segments of cerebral falx were obtained with region-growing and thresholding algorithms, and then a spline was fitted to maximize the symmetry between both sides of it. Elastic deformation was applied to the compressed hemisphere to 'pull' the midline back, then the mirror image was pasted to the lesion side. A morphing algorithm was then executed with control lines set at midline, the internal capsule, ventricular walls and outline of the hematoma.

RESULTS: This method was applied to a CT slice obtained from Neurosurgery online database. A multi-GIF image showing the transition from normal to abnormal image was generated. Shift of each pixel can be mapped in terms of magnitude and direction.

CONCLUSION: This method is useful for depicting shift of each brain structure in addition to midline, and can be applied to single or serial images. It is easily implemented on personal computers.

Keywords: Midline shift, Image morphing, Personal computer

INTRODUCTION

Symmetry is an important feature of biological images. The human brain appears bilateral symmetric and has corresponding anatomical structures of similar size and shape on both sides of the midline. Although some of these structures differ functionally, the normal hemisphere provide a age-matched control, whose image aids in manual evaluation of the diseased hemisphere by mentally reconstructing the relevant position of the displaced structure. Even with external compression, the unaffected hemisphere often has better anatomical detail compared to the diseased area. Therefore, midline shift remains one of the most commonly used neurosurgical jargon since the invention of brain imaging. To use this information on automatic evaluation of brain images, the displaced midline must be found first. However, applying symmetry criteria to brain imaging is not easy as it appeared. Finding the symmetry plane by calculating the principle axis of inertia fails in most occasions [8]. There have been a few reports discussing the computation of the normal midsagittal plane with volumetric MRI [4, 8]. None of them could trace the distorted midline. The author has developed a simple method of generating the midline with five control points with a personal computer, commercially available software, and an image obtained from Neurosurgery online database. After the shifted midline was found, it was straightened back. Image morphing [1] was utilized to generate an image sequence to illustrate the transition from the reference image to the pathological image.

MATERIALS AND METHODS

Equipment

Compaq Presario 5716 with Windows 98 OEM Version (Compaq Computer Taiwan Limited, Taipei, Taiwan) and its built-in programs

Material

A slice of CT image, MVC-033f.jpg (Figure 1A), from a patient with intracerebral hematoma was obtained from the previous version of Neurosurgery online image database (http://www.neurosurgery.org/nsimages, now at the new Web site http://www.neurosurgeon.org/nsimages)

Methods

The image was resized into 160x240 pixels and the grey levels reduced to 16 to facilitate QuickBASIC programming (Figure 1B). The skull was extracted from the image with region-growing algorithm and the area outside it was discarded. The distorted midline is divided into three segments: the upper and the lower segments of the falx, and the curved middle segment between them. The formers are firmly connected to the skull and usually appear as a straight line on CT. To define a curve, at least three points are required. The end points of the curved central segment of the midline are the end points of the two falx segments. Therefore, one or more additional points are required.

The upper and the lower segments of the falx were extracted from the image with region-growing algorithm, starting from the thickest portion of the skull, and gradually lowering the threshold. The best threshold resulting in the thinnest falx segment, i.e. the largest length/width ratio, was chosen. The end points of both falx segments are depicted and two line segments are drawn to transform the falx segments into straight lines (the blue lines in Figure 1B).

To select the third point defining the curve, a window, bounded by the Y-coordinate of the two end points and one half of the width of the brain image, was created. An exhaustive search was performed to locate the best-fitted curve. In this report, a quadratic Bezier curve, $P(x, y) = t^2 A(x_1, y1) + t(1-t) B(x_2, y2) + (1-t)^2 C(x_3, y3)$, $t = 0$ to 1, was used but a quadratic function depending on the Y-coordinate is also acceptable in many occasions. However, when the maximal shift is not around the midpoint of the curve, a higher order curve is required, and the processing time will increase markedly.

Symmetry was computed as the sum of squares of the intensity difference for pixels within a predefined window around the point. For global symmetry around a curve, this was done by simply adding the difference along each horizontal line segment. If significant tilting is present in the original figure, rotation is required for further processing. Summation of difference along the normal seems to be a more accurate way, but it is slower and always generated almost the same result because of the large number of points considered. The curve with best symmetry, i.e. the smallest intensity difference between two sides in its proximity, was selected as the central segment of the midline, and was plotted on the original figure (the red curve in Figure 1B).

After finding midline, a normal image can be generated, assuming the normal hemisphere is only compressed, and pulling the midline back would return it into the normal configuration. Thereafter, the mirror image of the normalized hemisphere is pasted on the lesion side, completing the ‘normal’ reference image (Figure 1C).

To perform the morphing action, matching features should be selected first. This is done by segmenting both the pathological and the reference images, depicting the skull, the superficial white/gray matter, the basal ganglia including the internal capsule, the ventricles, the hematoma and the area of perifocal edema. For high-contrast areas like the skull, the hematoma and the ventricles, the process is straightforward. Thresholding and region growing suffice. For low-contrast areas, such as the internal capsule, a priori information and some processing with mathematical morphology are required. The author use a small program to search for low-density line segments originating around the posterior margin of the frontal horn, trying to find the anterior limb between the caudate and the lenticular nucleus, and the posterior limb between the thalamus and the lenticular nucleus.

Areas that disappeared, arisen *de novo*, or fragmented, required special attention. The intracerebral hematoma was not seen in the reference image, and the right occipital horn disappeared on the pathological image. Furthermore, the right frontal horn on the pathological image appeared segmented by the displaced caudate nucleus, and the manually depicted smaller segment had shape and density similar to the surrounding small areas of perifocal edema.

Matching the control points/lines is a labor-intensive work still done by human experts in most morphing tasks, as is in this report. The midline is straightened, rotating the deviated segments of falx into midline and straightening the curve in between. The internal capsule is returned into its position in the ‘normal’ image. The intracerebral hematoma is shrunk into its center. The right frontal horn was “inflated”, and the right occipital horn was also “inflated” from its most medial and anterior point in the ‘normal’ image.

A simplified version of elastic deformation transformation [2] is performed to compute the displacement of other points in the original figure. The process can be regarded as a complex form of interpolation. For pixels without corresponding points in the original image, points of the reference image were inserted. Finally, the hypodensity of the perifocal edema was normalized, completing the process of transformation. The in-between images were easily computed by applying fractions of the deformation field to the original image.

RESULTS

The deformed midline was successfully traced in this image (Figure 1B) and was straightened to simulate a “normal” image (Figure 1C) as a reference for the calculation of brain shift.

The displacement field was generated by applying elastic deformation algorithm to the image pairs of Figures 1B and 1C. The direction and angle of displacement was calculated and visualized (Figure 2). The shift is propagated through the ipsilateral basal ganglia into contralateral basal ganglia. Significant compression is noted on the occipital and frontal horns of the lesion side, but not on the normal side. The area of ipsilateral white matter is increased, but that of contralateral white matter is decreased. The size change of basal ganglia is less pronounced.

The morphing process is shown in Figure 3.

DISCUSSION

Automatic segmentation of brain structures is not always an easy task on MRI, which has multiple pulse sequences and relatively good tissue contrast. It is even more difficult in the more commonly encountered CT scans not done for volumetric or image guided interventions. However, human experts perform evaluation of this type of information considered ‘difficult’ for machine interpretation. Symmetry is an important reference. We often compare the ‘abnormal’ hemisphere to the normal one, trying to find where the deformed structure is located, rather than referring to the atlas directly. Furthermore, matching the severely distorted image directly to the atlas cannot differentiate the chronic (degenerative) change from the acute pathology without additional information. If the pathology is unilateral, the above strategy could be applied after midline found and its shift reversed.

The cerebral falx, the third ventricle and septum pellucidum form the midline in the supratentorial compartment. Identifying these structures effectively define the midline when there is no mass effect. Therefore, any algorithms capable of tracing the hyperdensity in the interhemispheric fissure can identify the midline in any single slice of CT scan. When the falx is deviated, it could still be identified in the same way unless there is hyperdense interhemispheric blood. However, this is not the case for the ventricular system, where partial or total collapse may occur in addition to displacement. Midline in this area is best defined by the paired periventricular structures such as the frontal horns and the thalami.

Most midline-finding algorithms tackle the problem in two steps. First, some landmark points are picked out using various filters and thresholding. Edges [4], ridges [8], or specific tissue classes are identified. Next, a plane achieving best bilateral symmetry between these landmarks is identified. The former step fails when the deformation is large enough to reduce the number of points in one side but not the other, especially in the early stage of image processing, when the information regarding tissue class is not available. In this report, comparison of the intensity of the pixels without classifying them is the key to obtaining enough samples while avoiding the error generated by misclassification. However, with significant intensity change near the midline, such as thalamic or intraventricular hemorrhage, this method also generates incorrect response. Regarding the search process, exhaustive search is still required if there is significant distortion of the image. Whether there are any shortcuts to prevent local maxima remains unknown.

An important characteristic of the algorithm in this report is simplicity and thus large potential for application. There is no need for three-dimensional volumetric data as well as a large number of slices containing only normal anatomy, which may be regarded as trivial for human recognition and discarded. Any slice of CT or MRI image from an archive, database, or website, such as the Neurosurgery Online Database, can be retrieved and processed. Midline was successfully traced in other single slice images with various data format, and some even resized. The downsized image transmitted by mobile phone [10] is also suitable for this method, and a simple version of midline finder may be installed. Some preprocessing by mathematical morphology may be required for resized images or those reconstructed with lossy compression algorithms such as JPEG.

Whatever the method used, the traced midline may be used to calculate midline shift as clinicians do. Furthermore, it aids in tissue classification, which is difficult in the presence of significant brain shift, and can be incorporated into an iterative process to further fine-tune the identified midline. When the third ventricle is collapsed, the medial boundary of the thalami, which cannot be identified otherwise due to the same density of homologous structures, is the traced midline. The problem of assigning the midline of the corpus callosum is solved in the same way. Mapping the boundary of homogeneous areas (such as the outline of both thalami) rather than just blindly relying on open curves may improve the performance of registration algorithms.

When computing the deformation field in this report, considerable human intervention is still required. Building a disease-specific database may be useful, but a large storage space might be required for different pathologies. From the deformation map, as well as on the first look, we can see that the ventricle on the lesion side underwent large deformation, as well as superficial gray matter and white matter near the lesion. The basal ganglia had less significant size change. They seemed to “transmit” the stress to other structures. These phenomena and the configuration of the shifted midline may reveal the difference of the mechanical properties between different types of intracranial structures. The model proposed by Nagashima [6] emphasized the difference between gray and white matters. As its successor, the fixation of falx segments is also considered in Pena et al’s report [7]. It is interesting to know the behavior of these models if unilateral rather than bilateral ventricular dilatation occurs.

The morphing process was generated by applying fractions of the shift to the original image. It is good for visualization or demonstration, but far from modeling, however. A simple gradient along one direction such as that appeared in [9] is rarely observed clinically in pathological scans. Intraoperative motion of different tissue at different position assumes various direction and magnitude, and is almost unpredictable by present model [3]. Nabavi et al. [5] has pointed out that brain shift does not occur simultaneously, and many intraoperative images are not in steady state. For image pairs in longer intervals, such as weeks, months, or even years, the morphing might be a better approximate of the real process.

CONCLUSION

The author has proposed an automatic method for tracing the midline on a slice of brain CT. This method is useful for depicting shift of each brain structure in addition to midline, and can be applied to single or serial images. It is easily implemented on personal computers and helps with visualization of lesion formation.

REFERENCES

1. Anderson S: Morphing Magic. Carmel, Indiana, SAMS publishing, 1993.
2. Davatzikos C, Prince JL, Bryan RN: Image registration based on boundary mapping. IEEE Transactions on Medical Imaging 15: 112-5, 1996
3. Keles GE, Lamborn KR, Berger MS: Coregistration accuracy and detection of brain shift using intraoperative sononavigation during resection of hemispheric tumors. Neurosurgery 53:556-564, 2003.
4. Liu Y, Collins RT, Rothfus WE: Robust midsagittal

plane extraction from normal and pathological 3-D neruoradiology images. IEEE Transactions on Medical Imaging 20: 175-192, 2001.
5. Nabavi A, Black PM, Gering DT, Westin C, Mehta V, Pergolizzi RS, Ferrant M, Warfield SK, Hata N, Schwartz RB, Wells WM, Kikinis R, Jolesz FA: Serial intraoperative magnetic resonance imaging of brain shift. Neurosurgery 48:787-798, 2001.
6. Nagashima T, Tamaki N, Matsumoto S, Horwitz B, Seguchi Y: Biomechanics of hydrocephalus: a new theoretical model. Neurosurgery 21: 898-904, 1987.
7. Peña A, Bolton MD, Whitehouse H, Pickard JD: Effects of brain ventricular shape on periventricular biomechanics: a finite-element analysis. Neurosurgery 45:107-118, 1999.
8. Prima S, Ourselin S, Ayache N: Computation of the mid-sagittal plane in 3D brain images. IEEE Transactions on Medical Imaging. 21:122-138, 2002.
9. Warfield S, Robatino A, Dengler J, Jolesz F, Kikinis R: Nonlinear registration and template driven segmentation, in Toga A (ed): Brain Warping. San Diego, Academic Press, 1998.
10. Yamada M, Watarai H, Andou T, Sakai N. Emergency Image Transfer System Through a Mobile Telephone in Japan: Technical Note. Neurosurgery 52:986-990, 2003.

FIGURES

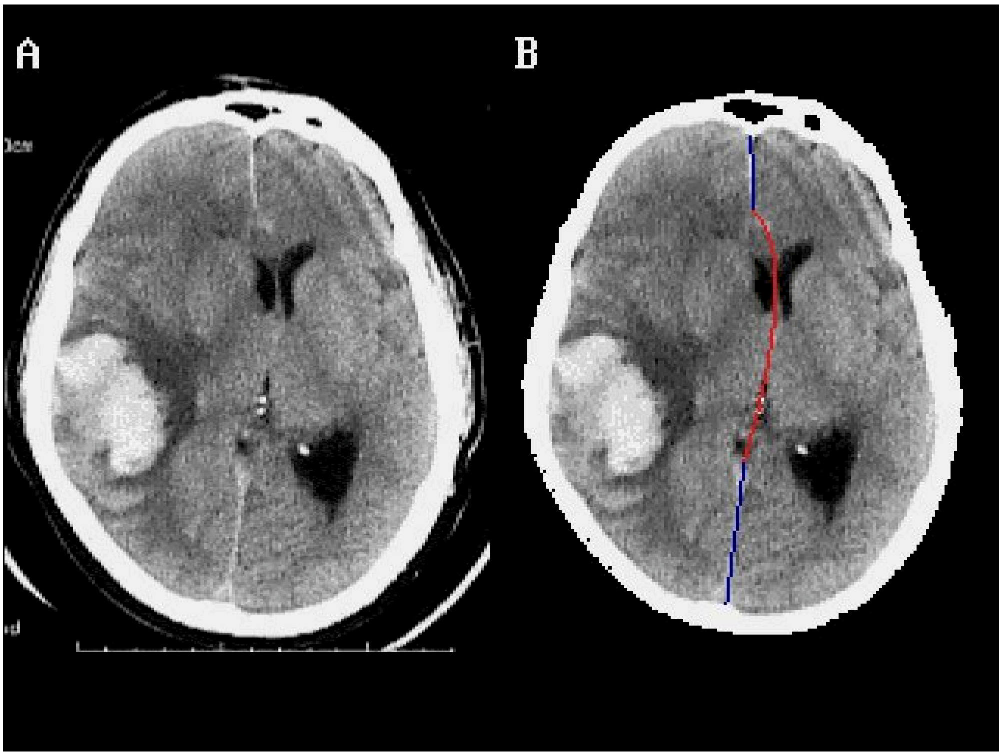

FIGURE 1. A slice of brain CT from Neurosurgery online database showing intracerebral hemorrhage A: the original image, 312 x 375 pixels, JPEG format; B: the reformatted image (160 x 120 pixels, 16 grey levels) with upper and lower segments of falx (blue) segmented with region growing algorithm and the central segment (red) formed by a Bezier curve (see text); C: the "normal" reference image formed by straightening the midline and expanding the normal (left) hemisphere, then paste the mirror image on the affected (right) side.

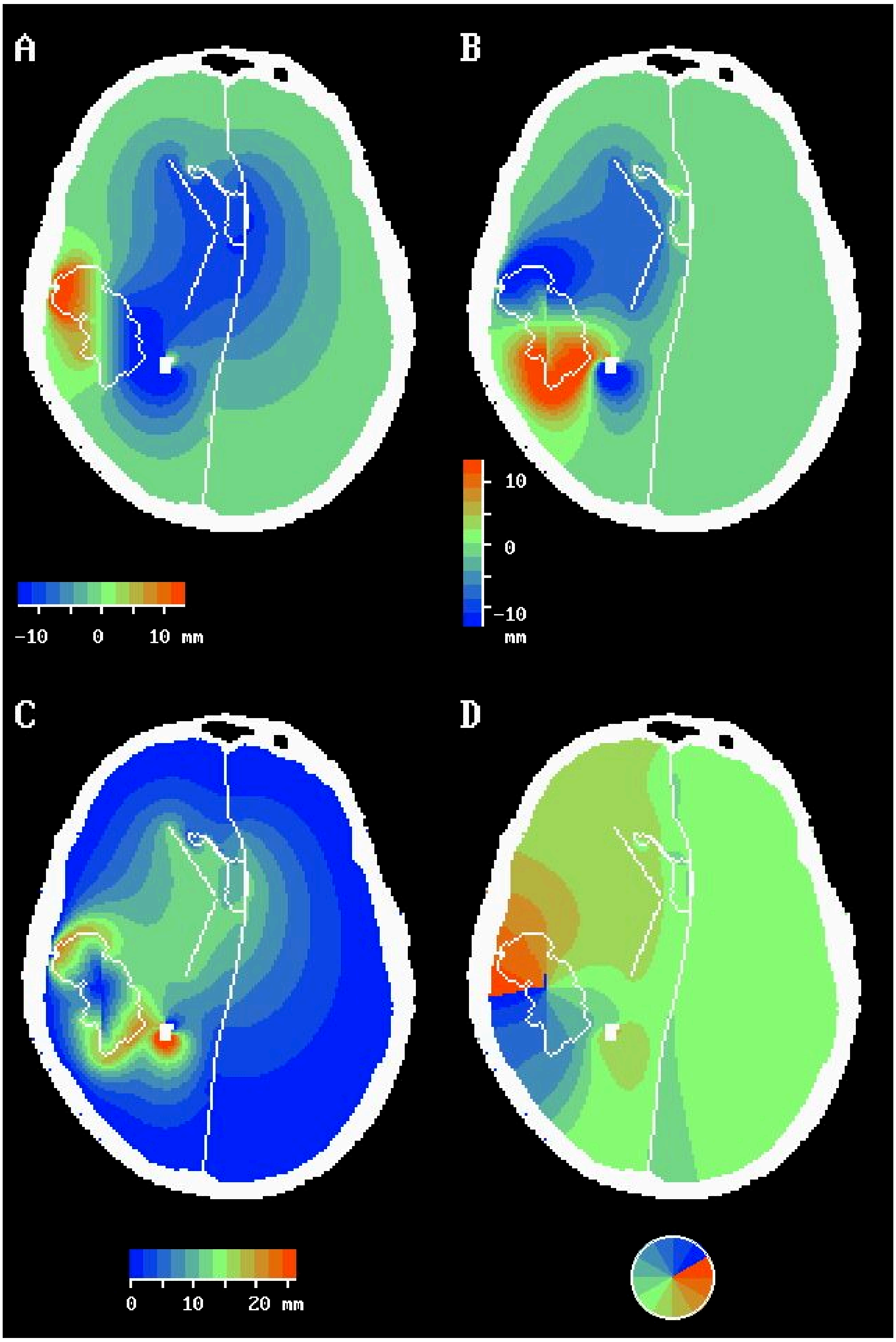

FIGURE 2. The displacement of each points in Figure 1B along the X-axis (A) and the Y-Axis (B) calculated by elastic transformation after picking out the control points (the hematoma, the internal capsule, and the ventricles, shown in white). The magnitude (C) and direction (D) of the displacement can be calculated easily.

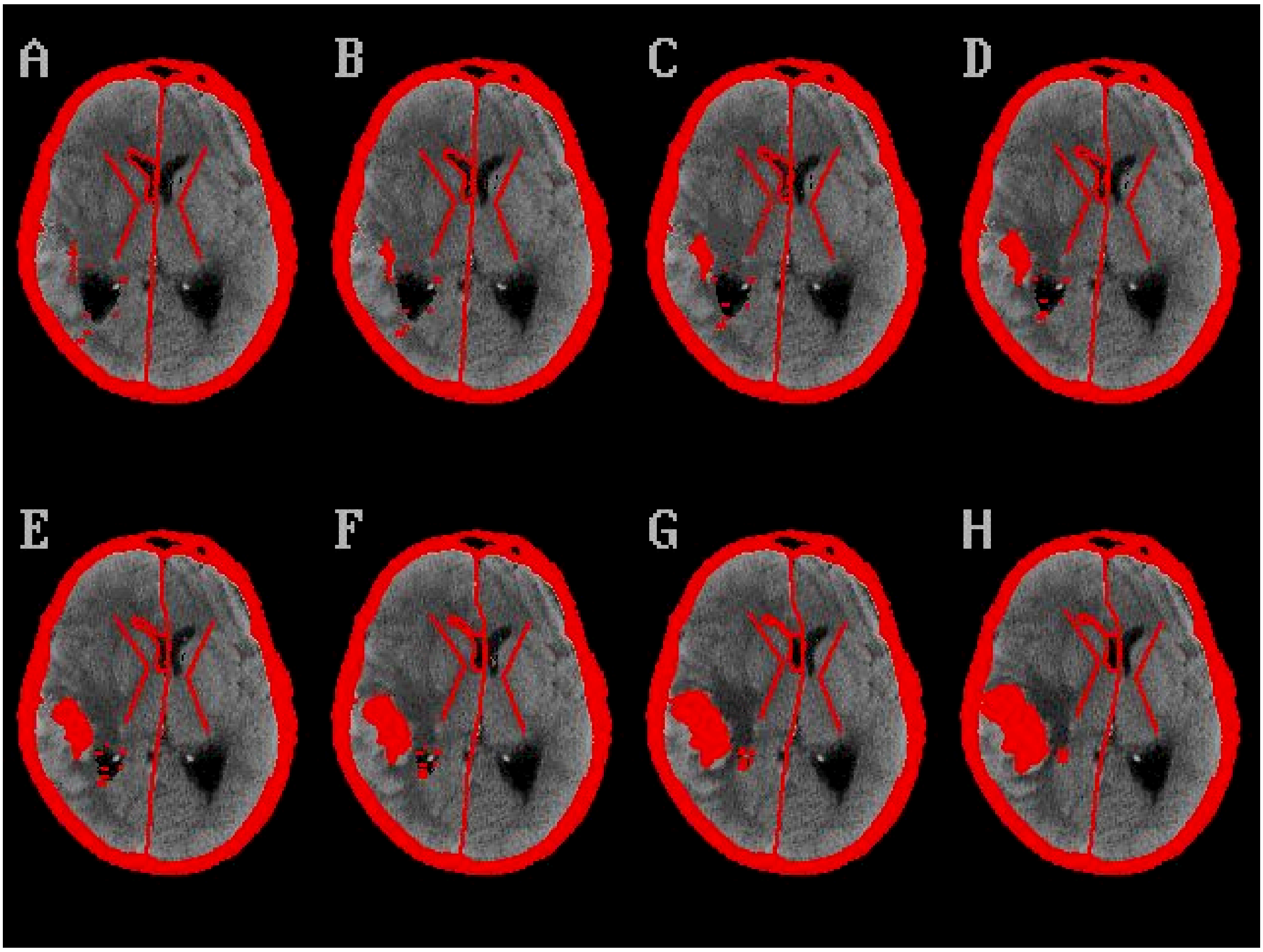

FIGURE 3. Sequence of the morphing process from the original image (H) to a “normal” one (A), much like Figure 1C. The control points are shown in red. A multi-GIF file can also be constructed for better visualization.